RESPONSE OF RESONANT TARGETS TO BROADBAND SIGNALS.

A.J. Fenwick[1] , D.Butler[2]

[1] UPS/FST, QinetiQ, Winfrith Technology Centre, Dorchester, DT2 8XJ, ajfenwick@qinetiq.com
[2] Thales Underwater Systems, Templecombe, Somerset, BA8 0DH, david.butler3@virgin.net

1. INTRODUCTION

When an active signal processing system is being designed, it is frequently assumed that the echo is comprised of returns from surface highlights and can be modelled as the sum of delayed and attenuated replicas of the signal. For some targets and some operating frequencies, the model is invalid either because the target has been set vibrating by the pressure wave, for example fish swim bladders or the signal travels around the target, and adds to the direct echo as in for example, wrecks. In such cases, a better model is the sum of a perfect reflection from a rigid or soft boundary and an elastic response.

A single resonance can be modelled as a second order linear filter with an infinite impulse response. The highlight model has a finite impulse response. As was found from research on the linear filtering of chaotic time series at RSRE Malvern in the early 90's, the two different types of filter produce distinct effects. Some properties of the input are not recoverable with the IIR filter [1]. Building on this, it was conjectured on the basis of arguments from non-linear dynamics, that when a resonant target is excited by a chaotic signal it would produce bursts of energy at apparently random intervals [2]. Numerical experiments established that bursting does occur [3], and afterwards it was observed in electrical and acoustic signals in ultrasonic experiments [4,5].

A natural question to ask is how this behaviour compares with the response to frequency modulated and pseudo-random noise signals. A partial answer is given below. In seeking to understand the causes and characteristics of chaotic bursting, an interpretation of the dynamical systems explanation in terms linear systems theory has emerged.

The next section introduces the signal types used and discusses issues which arise in carrying out the numerical experiments. It then shows the resonant response to LFM, PRN and chaotic signals. The implication for detection and classification are discussed in section 3. An analytical model for chaotic bursting is developed in section 4.

2. SIMULATED RESPONSES TO CHAOTIC AND STANDARD SIGNALS

2.1 Signals considered

Chaotic signals are generated by non-linear systems which are sensitive to initial conditions, by which two solutions starting from nearby points diverge as time increases. The signal used here is generated by the Duffing oscillator

$$\ddot{y} + b_d \dot{y} - y + y^3 = F\cos\omega t \ . \qquad \textbf{(1).}$$

As will be seen, chaotic signals have broadband spectra, comprising both lines and continuous components. Two conventional sonar signals with broadband spectra are linear frequency modulated carriers and pseudo-random noise. White pseudo-random noise is generated as a sequence of uncorrelated random numbers. To model the effect of the amplifiers and transducers,

this sequence is averaged using a moving window to give a triangular correlation function with a $(\sin x/x)^2$ spectrum at baseband which is used to modulate a carrier. The LFM signal is given by

$$y(t) = \cos(\omega_0 t + \beta t^2 + \phi), -T/2 \le t < T/2 \qquad \textbf{(2)}$$

Examples of this signal with unit power signals are shown in fig 1. For the Duffing signal, b_d = 0.3, F = 0.5, Ω = *1.2 rads/s*. For the PRN signal, the carrier frequency is ω_o = *0.4*, and for the LFM signal, ω_o = *0.4*, β =*8x10^{-5}/π* , ϕ = *0*. In each case, *T = 100*2π/ω_o*.

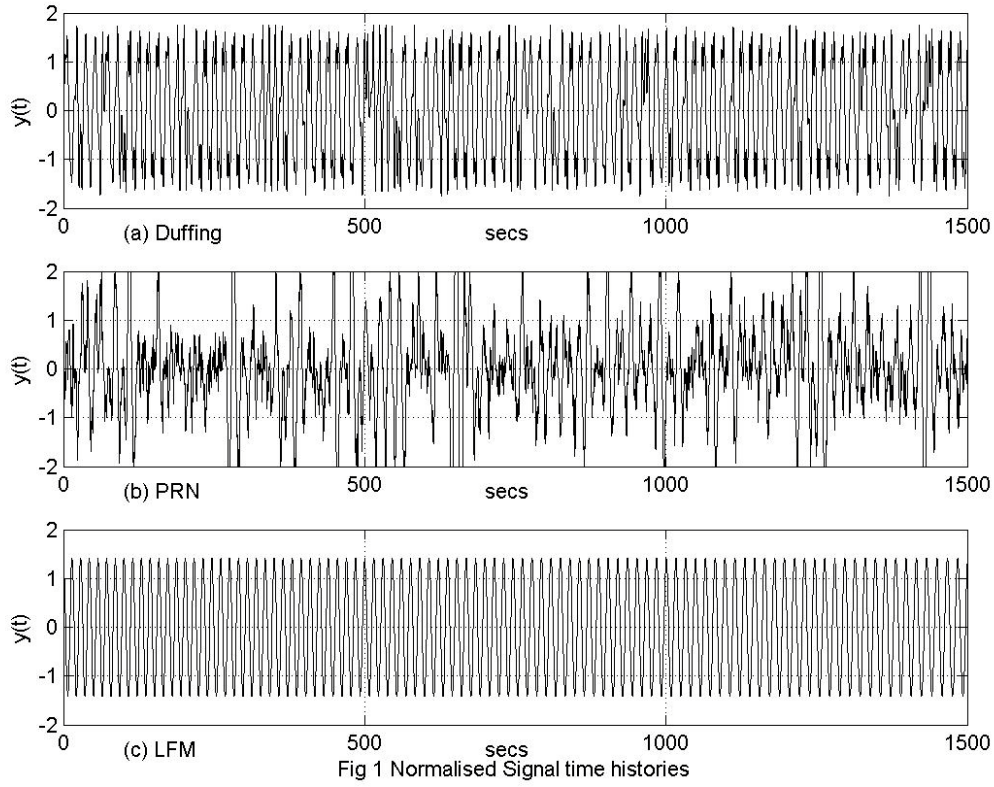

Fig 1 Normalised Signal time histories

2.2 Calculating the elastic response

The simplest case of an elastic response is a driven mass-spring oscillator. If *y(t)* is the signal and x*(t)* is the echo, then

$$\ddot{x} + b\dot{x} + kx = y(t) \qquad \textbf{(3)}$$

where *b* and *k* are the damping force per unit velocity and restoring force per unit displacement respectively. Representations which are equivalent to (3) are convolution in the time domain using the target impulse response *g(t)*,

$$x(t) = \int_0^t g(t-\tau)y(\tau)d\tau \qquad \textbf{(4)}$$

and in the frequency domain, using the target transfer function $G(\omega)$ with the Fourier transforms of $x(t)$, and $y(t)$ given by $X(\omega)$ and $Y(\omega)$

$$X(\omega)=G(\omega)Y(\omega) \qquad \textbf{(5)}$$

From (3),

$$G(\omega) = 1/(-\omega^2 + ib\omega + k) \qquad \textbf{(6).}$$

When the oscillator is underdamped, (6) has a peak at approximately $\omega_r = \sqrt{k - b^2/2}$ and *3 dB* bandwidth of $\Delta\omega = \sqrt{k^2 - \omega_r^4}/\omega_r$. The quality factor *Q* is $\omega_r/\Delta\omega$.

In calculating the response, any of these representations may be used. The chaotic signal is found by integrating the differential equation shown in (1), and (3) is the most convenient.

2.3 Comparison and discussion of behaviour

To demonstrate bursting, the resonant responses of a target with a resonance at ω_r = *0.4 rad/*s and a quality factor of *Q* = *50* are calculated. These are shown in fig 2. . It should be emphasised that these plots are samples from aperiodic oscillations and much different behaviour may be observed in different observation windows.

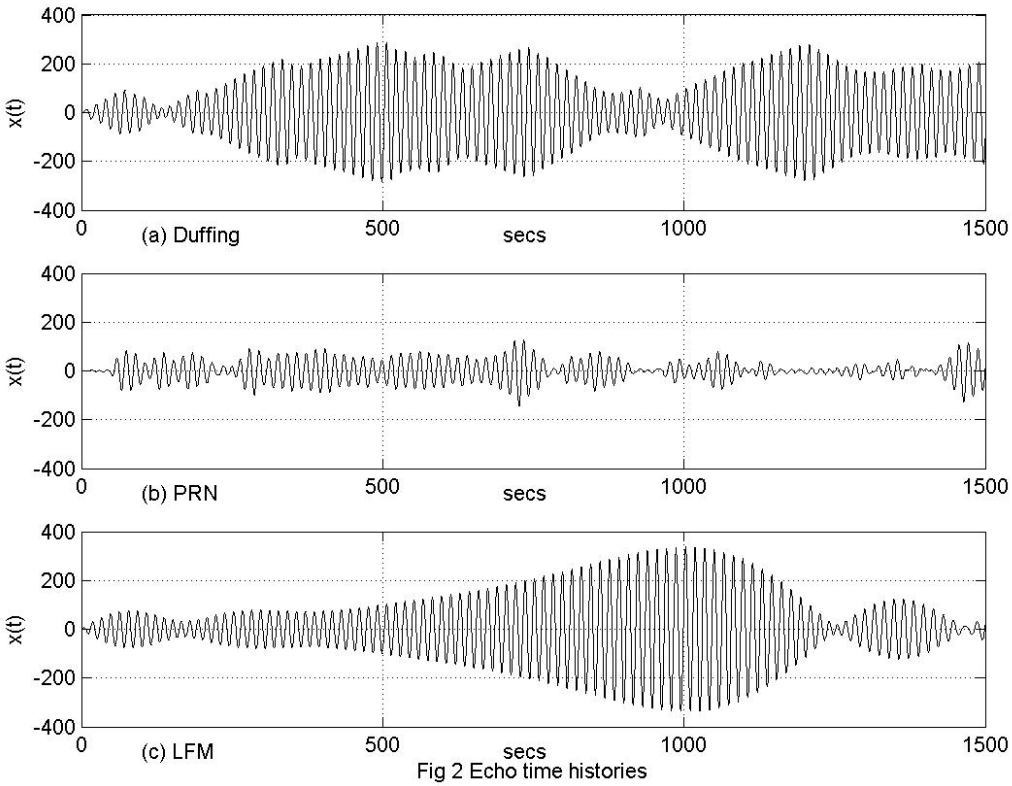

Fig 2 Echo time histories

The response to the Duffing signal behaves in a complex manner. There are regions where the envelope ramps up or down, e.g. near *t = 500*. Near *t = 0*, there may be beats. The PRN response also shows short term increases in energy. For the LFM drive, the output envelope increases to a maximum which is preceded and followed by beats. These results can be better understood by referring to the spectra for the signals shown in fig 3. Note that the spectra for the Duffing and PRN signals are averaged over eight subwindows to reduce fluctuations.

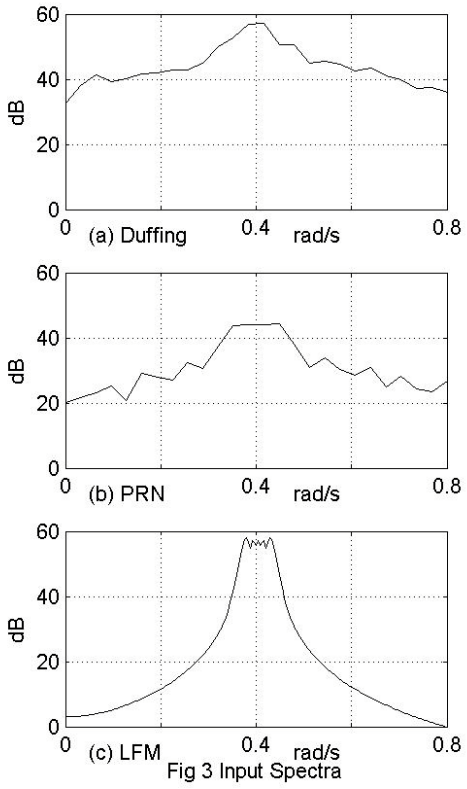

Fig 3 Input Spectra

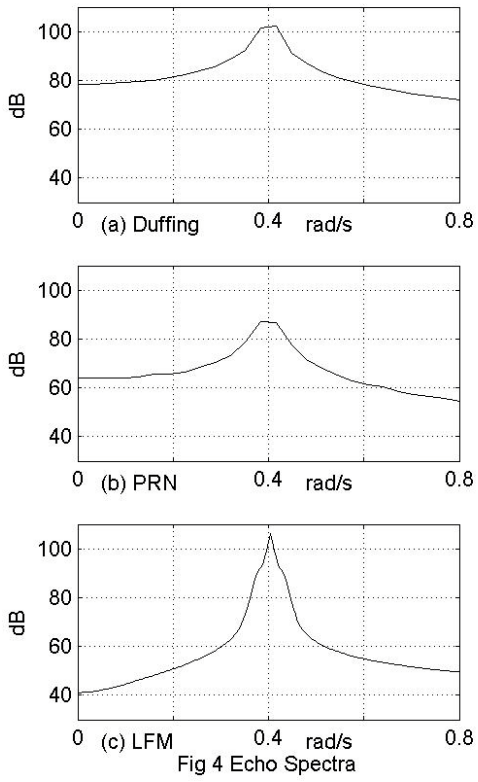

Fig 4 Echo Spectra

The target resonance lies within a plateau in each of the spectra, hence there is a strong signal component at the target resonant frequency. The envelope fluctuations may reasonably be related to the response of a linear oscillator being driven at its resonance. None of the responses reaches a steady state, because, referring to fig 1, the signal changes frequency or phase too frequently. The peak value and the times to reach it are related to the Q of the resonance.

In fig 4, the spectra of the echoes are plotted. Those for the Duffing and PRN signals are averaged over eight subwindows. The target transfer function *G(f)* is highly peaked and (5) suggests that the echo spectra will have a peak at the resonance. Fig 4 shows this is the case.

2.4 Multiple Resonances

When there is more than one resonance, each will cause bursting at a level determined by the spectrum of the input signal and the Q of the resonance. Each contribution will add or subtract from the others. The resultant envelope may have much larger excursions or much smaller ones than for a single resonance and be very complex overall.

3. IMPLICATIONS FOR PROCESSING

The first problem is to detect the echo and the first choice for processing is to cross-correlate the returns with a copy of the signal. For a point target in stationary white noise, this produces the maximum signal-to-noise ratio, and is statistically optimum in Gaussian noise. For coloured noise, or a more complex target which produces a modified waveform, there will be a correlation loss. Fig 5 shows the result of cross-correlating the echo from with the signal in each case. The maximum correlation is less than 1, thus the signal-to-noise is reduced, the peak is shifted from zero relative lag and there is an error in range determination.

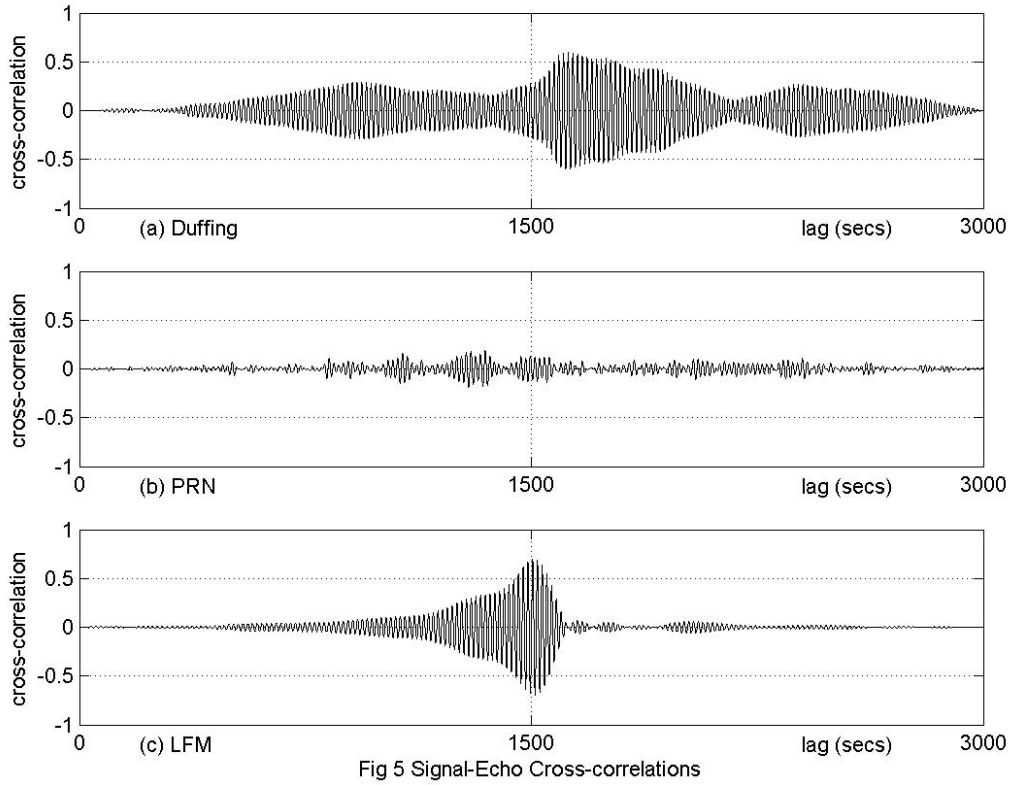

Fig 5 Signal-Echo Cross-correlations

The loss may be recovered if the signal copy is adjusted to account for the target response. For an unknown response, a set of filters, each matched to a particular target, can be used. This principle allows a target with multiple resonances to be detected. By analogy with high range resolution processing, where the echoes from multiple highlights may be resolved using a signal with sufficient bandwidth, a long enough window would allow high frequency resolution processing to resolve resonances.

If the signal-to-noise ratio is high enough, a direct estimation of the target impulse response or transfer function might be attempted. This is a system identification problem. If analysis is performed in the frequency domain, the target transfer function is estimated by finding the ratio between the received spectrum and signal spectrum. A method of non-linear system identification [6] has been shown to be capable of extracting the centre frequency and bandwidth of a linear filter driven by a chaotic signal [7].

4. ANALYTICAL MODEL FOR CHAOTIC BURSTING

If the Duffing waveform is examined closely, it appears to be constructed from sections of periodic oscillation, punctuated by rapid changes. A model for the bursting resulting from this behaviour can be constructed by assuming that the signal comprises sine wave sections each with constant amplitude, frequency and phase, but switching one or more at the start of the next section [8]. This simple model produces all the types of behaviour seen in chaotic bursting.

4.1 A linear oscillator with input discontinuities

Consider a simple damped oscillator with unit mass, damping b and spring stiffness $k = \omega_0^{\,2}$. Let the displacement and velocity at time *t* be $x(t)$ and $\dot{x}(t)$. Consider a drive comprised of *N* sections such that the $i'th$ section lasting from time t_i to t_{i+1} is a cosine wave with amplitude a_i, angular frequency Ω_i and phase ψ_i. The response of the system is given by

$$\ddot{x} + b\dot{x} + \omega_o^2 x = \sum_{i=1}^{N} W\left(t_i, t_{i+1}, t\right) a_i \cos\left(\Omega_i\left(t - t_i\right) + \psi_i\right) \qquad (7)$$

where $W(t_i, t_{i+1}, t) = 1$ for $t_i \le t < t_{i+1}$

$= 0$ *otherwise* (8)

with initial conditions $x(t_1) = X$ and $\dot{x}(t_1) = U$. A clearer understanding emerges if the response of undamped systems is considered first.

4.2 Behaviour of an undamped oscillator

Two cases will be studied, the first when the sine wave drive frequency is equal to the filter resonance and the second when it is offset from the resonance. The filter resonant frequency is ω ad/s. The other quantities are as just defined, dropping the subscripts. It is only necessary to consider the behaviour of the filter response with a single section of drive.

When $\Omega = \omega$, the system equation is

$$\ddot{x} + \omega^2 x = a\cos(\omega t + \phi) \qquad (9)$$

with initial conditions $x(0) = X$, $\dot{x}(0) = U$. The envelope $E(t)$ of x(t) is given by [8]

$$E^2(t) = \left(\frac{at}{2\omega} + \frac{\cos\phi}{\omega}\left(U - \frac{a\sin\phi}{2\omega}\right) + X\sin\phi\right)^2 + \left(X\cos\phi - \frac{\sin\phi}{\omega}\left(U - \frac{a\sin\phi}{2\omega}\right)\right)^2 \qquad (10)$$

The solution holds for $0 \le t \le T$, where T is the length of time for which the drive is applied. The second term in brackets is independent of time, and the square of the envelope is a hyperbola with axes *t = 0* and *E = 0*. If the combination of parameters is such that the second bracket vanishes, the hyperbola degenerates into a pair of straight lines. When the drive term changes (ϕ or a changes), a change is initiated in the envelope which depends on the values of *x* and *dx/dt* at the time of the change.

When $\Omega \ne \omega$, the system equation is

$$\ddot{x} + \omega^2 x = a\cos(\Omega t + \phi) \qquad (12)$$

with initial conditions $x(0) = X$, $\dot{x}(0) = U$. With frequency difference, $\delta\omega = \Omega - \omega$, the envelope $E(t)$ is given by (see [8]):

$$E^2(t) = M^2 + C^2 + 2MC\cos(\delta\omega.t + \phi + \psi) \quad \textbf{(13)}$$

where $$M^2 = (X - C\cos\phi)^2 + \frac{1}{\omega^2}(U + \Omega C\sin\phi)^2 \ , \ C = a/\omega^2 - \Omega^2 \quad \textbf{(14)}$$

and $$\sin\psi = (U + \Omega C\sin\phi)/\omega M \ , \ \cos\psi = (X - C\cos\phi)/M \quad \textbf{(15)}$$

The only time varying term in (10) is the last and the envelope is modulated by a beat frequency.

4.3 Behaviour of a damped oscillator

The system equation is

$$\ddot{x} + b\dot{x} + \omega_o^2 x = a\cos(\Omega t + \phi) \quad \textit{with} \quad x(0) = X, \dot{x}(0) = U \quad \textbf{(16)}$$

The envelope $E(t)$ of the solution is given by:

$$E^2(t) = e^{-bt}H^2 + K^2 + 2e^{-\frac{bt}{2}}HK\cos(\delta\omega.t + \phi + \psi) \quad \textbf{(17)}$$

where $$H^2 = A^2 + B^2, \quad K^2 = \alpha^2 + \beta^2 = \frac{a^2}{\{(\omega_0^2 - \Omega^2)^2 + b^2\Omega^2\}}, \quad \textbf{(18)}$$

$$A = X - (\alpha\cos\phi + \beta\sin\phi), \quad \textbf{(19)}$$

$$B = \frac{1}{\omega}(U + \Omega(\alpha\sin\phi - \beta\cos\phi)) + \frac{b}{2\omega}(X - (\alpha\cos\phi + \beta\sin\phi)) \quad \textbf{(20)}$$

$$\alpha = D(\omega_o^2 - \Omega^2), \ \beta = Db\Omega, \ \cos\psi = \frac{A\beta + B\alpha}{HK}, \ \sin\psi = \frac{A\alpha - B\beta}{HK}. \quad \textbf{(21)}$$

$$D = a/\{(\omega_0^2 - \Omega^2)^2 + b^2\Omega^2\} \quad \textbf{(22)}$$

It follows that $E(t)$ lies within the bounds $|e^{-\frac{bt}{2}}H \pm K|$. The first term depends on the initial conditions, and the second on the drive frequency and the resonant frequency. As time increases the initial conditions are forgotten as can be seen from (17), and the envelope oscillates at a beat frequency as it decays to a constant level. At each change of the driving force *(Ω, ϕ* or *a*) a new envelope will arise, which may be larger or smaller than the previous one. It should be noted that the envelope is determined by the initial conditions X or U, and also by α, β, ϕ and Ω.

4.4 Numerical examples

Fig 6 shows the responses of two resonant targets to a switched sine wave. The first is as before, ω_r = *0.4 rad/s* Q = *5*0 and for the second ω_r = *0.4* with no damping. These are labelled 1 and 2

respectively. In figs 6(a) and (c), the effects of suddenly increasing signal phase by $3\pi/4$ at the resonant frequency are shown. In the undamped target (fig 6(a)), the envelope of the response is initially a pair of straight lines, but after each phase switch, the envelop is comprised of the two branches of a general hyperbola. The effect of the damping shown in fig 6(c) is to superimpose an exponential decay on the rises and falls, preventing growth without limit. In figs 6(b) and (d), the amplitude and phase are constant, but the frequency steps from *0.36* to *0.4* then to *0.44*. In fig 6(b), where there is no damping, the envelope initially shows beating at the difference $\omega_d - \omega_r$ between the drive and resonant frequencies. On switching the drive to the resonant frequency, the envelope grows in level until halted by the switch up in frequency. The third section shows a cosine modulation of a constant envelope at the difference frequency $\omega_d - \omega_r$. When there is damping, as shown in fig 6(d), the beats are smoothed out and the oscillation eventually decays to a level determined by the filter transfer function.

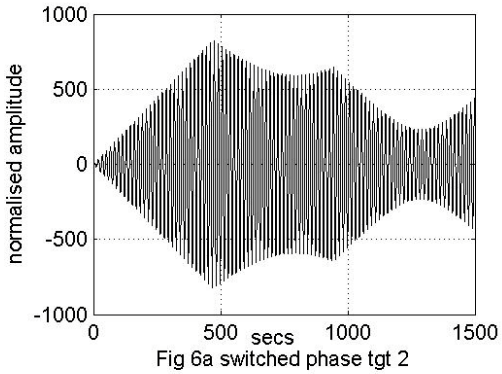

Fig 6a switched phase tgt 2

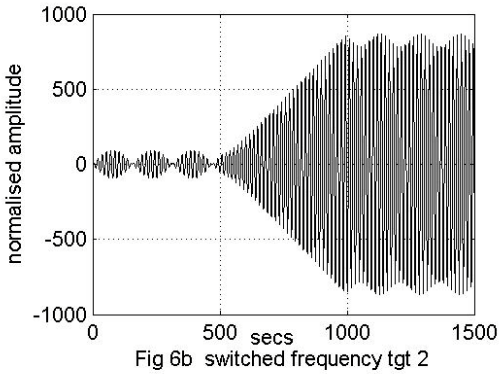

Fig 6b switched frequency tgt 2

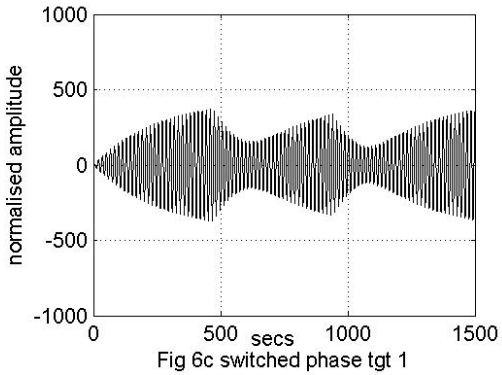

Fig 6c switched phase tgt 1

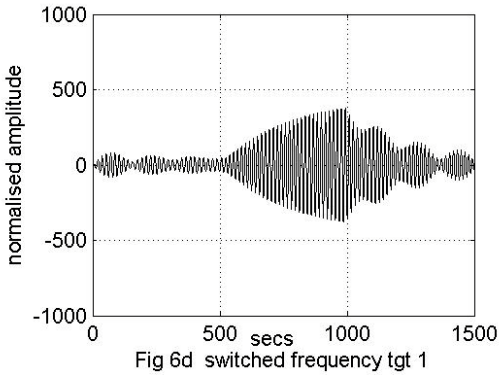

Fig 6d switched frequency tgt 1

Simulations with switches in amplitude produce changes in the slope of the envelope. The envelope always increases if the filter is undamped. With damping, a switch causes a short term increase which decays until the next change.

4.5 Non-linear dynamical systems theory explanation

The sudden changes in the chaotic Duffing signal associated with bursting in the echo are due to changes in the stability of the oscillator arising from the non-linearity. For a time, the oscillation is stable, but sooner or later, it reaches a combination of position and velocity for which the system becomes unstable, and a sudden change occurs as it seeks a new region of stability. This

behaviour has been studied for discrete time systems [9], was conjectured to hold for continuous systems [2] and has been demonstrated here. The loss in stability is associated with an increase in the so-called short-term Lyapunov exponent. The long-term Lyaponuv exponent measures the average rate at which two time series starting at nearby points diverge from each other. A precise definition requires careful attention to detail [10], but can be illustrated as follows. Consider $x(t,x_0)$ and $x(t,x_0+\delta x)$ which are two starting points for a system, and let the difference between the two at a later time $\Delta x(t) = |x(t,x_0) - x(t,x_0+\delta x)|$. While $\Delta x(t) << 1$, $\Delta x(t) \approx \Delta x(0)e^{\lambda t}$ where λ is the Lyapunov exponent. It should be noted that these arguments apply generally to any dynamical system and the switched sine wave model is also not restricted to the Duffing system.

5. CONCLUSIONS

Bursting can occur in the echo of a resonant target for noise-like broadband signals whose average spectra have significant energy near the resonance of the target. It was also shown to occur for sequences of sine waves with switched phase or frequency. There is a small correlation loss in the matched filtering of the bursting echoes considered.

REFERENCES

[1] Broomhead DS, Huke JP and Muldoon MR. Linear Filters and Non-linear systems. J Roy Stat Soc B Met 1992; 54 (2) : 373-382

[2] Broomhead DS. Private Communication. March 2000

[3] Fenwick AJ. Scattering of chaotic signals from simple resonant targets. QINETIQ/FST/TWP031922, July 2004

[4] Fenwick AJ, Adamson JE and Humphrey VF. Conference papers in bursting in Target Echoes. QinetiQ/FST/TR40954, Feb 2004

[5] Adamson JE, Fenwick AJ and Humphrey VF. Transmission of a chaotic signal through a flat plate. in Proceedings of the 7th European Conference on Underwater Acoustics, The Hague, 5-8th July 2004, in press

[6] Batchelor A. Modelling of Interconnected Nonlinear systems. Ph.D Thesis, Newcastle University, Newcastle upon Tyne, January 2004

[7] Batchelor A. Private communication. April 2004

[8] Fenwick AJ and Butler D. A study of bursting in linearly filtered chaos. QINETIQ/FST/TWP040339, July 2004

[9] Ashwin P and Ashton PJ. Blowout bifurcations of codimension two. Phys Lett A 1998 ; 244 :261-270

[10] Kantz H and Schreiber T. Nonlinear Time Series Analysis 2nd Ed.. Cambridge University Press, 2004, pp 65-69

ACKNOWLEDGEMENTS

This work was supported by the Sensors & Electronic Warfare Domain of UK MOD's Corporate Research Programme.